ELSEVIER

Journal of Controlled Release 69 (1999) 35–47

journal of controlled release

Comparison of the effects of short, high-voltage and long, medium-voltage pulses on skin electrical and transport properties

Rita Vanbever[a,b], Uwe F. Pliquett[a,c], Véronique Préat[b], James C. Weaver[a,*]

[a]*Harvard—M.I.T. Division of Health Sciences and Technology, Massachusetts Institute of Technology, Cambridge, MA 02139, USA*
[b]*Department of Pharmaceutical Technology, School of Pharmacy, Catholic University of Louvain, Brussels, Belgium*
[c]*Faculty of Chemistry, University of Bielefeld, Bielefeld, Germany*

Received 8 April 1998; accepted 12 January 1999

Abstract

High-voltage pulses have been shown to increase rates of transport across skin by several orders of magnitude on a time scale of minutes to seconds. Two main pulse protocols have been employed to promote transport: the intermittent application of short (~1 ms) high-voltage (~100 V across skin) pulses and a few applications of long (=100 ms) medium-voltage (>30 V across skin) pulses. In order to better evaluate the benefits of each protocol for transdermal drug delivery, we compared these two protocols in vitro in terms of changes in skin electrical properties and transport of sulforhodamine, a fluorescent polar molecule of 607 g/mol and a charge of −1. Whereas both protocols induced similar alterations and recovery processes of skin electrical resistance, long pulses of medium-voltage appeared to be more efficient in transporting molecules across skin. Skin resistance decreased by three (short pulses) and two (long pulses) orders of magnitude, followed by incomplete recovery in both cases. For the same total transported charge, long pulses induced faster and greater molecular transport across skin than short pulses. In addition, a greater fraction of the aqueous pathways created by the electric field was involved in molecular transport when using long pulse protocols. Transport was concentrated in localized transport regions (LTRs) for both protocols but LTRs created by long pulses were an order of magnitude larger than those formed by short pulses and the short pulses created an order of magnitude more LTRs. Overall, this study is consistent with the creation of fewer, but larger aqueous pathways by long, medium-voltage pulses in comparison to short, high-voltage pulses.

Keywords: Human skin; Electroporation; Electrical properties; Transdermal transport; Aqueous pathways

1. Introduction

Application of high-voltage electric field pulses to cells and tissue is believed to cause structural rearrangements within the lipid bilayer membranes such that transmembrane aqueous pathways are created [1,2]. According to this hypothesis, the electric field pulse plays the dual role of causing pore formation and providing a local driving force for ionic and molecular transport through the pores. The electrical conductance, permeability and molecular transport across lipid bilayers rapidly increase by many orders of magnitude, with these changes being reversible or irreversible depending on pulse parameters [1,2]. Electroporation of the stratum corneum

*Corresponding author. Tel.: +1-617-253-4194; fax: +1-617-253-2514. E-mail address: jim@geldrop.mit.edu (J.C. Weaver)

0168-3659/99/$ – see front matter
PII: S0168-3659(99)00018-8

(SC) lipid bilayers, the outermost layer of the skin, has been proposed as a mechanism to enhance transdermal drug delivery [3–7].

Transdermal drug delivery offers several potential advantages over conventional methods, such as the oral and injectable routes [8,9]. When compared to oral delivery, administration across skin avoids gastro-intestinal and first-pass liver degradation. When compared to the injectable route, it is non-invasive and has the potential to be a convenient and safe method of delivering drugs at steady or time-varying rates. However, the extension of passive transdermal delivery to a large number of drugs has been limited by the SC's natural barrier properties, attributed primarily to the intercellular lipids. Conventional passive transdermal therapy is only applicable to small, potent and lipophilic solutes. Chemical, electrical, ultrasonic and other methods of enhancement have been studied as approaches to increase the rates of transport [10].

Electroporation of skin has been shown to increase transport into and/or across skin for compounds ranging in size from small drugs, to macromolecules, to microspheres; ranging in charge from neutral to heavily charged; and in solubility from water-soluble to oil-soluble. Enhancement of transdermal transport by up to four orders of magnitude and onset times for transport of minutes to seconds have been achieved. Although most work has been performed in vitro, animal studies in vivo have shown similar results [5,6,11].

Electroporation experiments with skin have used exponential-decay electric field pulses that generate transdermal voltages between 50 and 100 V, and generally last for 1 to 2 ms [3,12–14]. Because the SC contains approximately 100 bilayer membranes in series, these conditions are well inside the range of pulse voltage and duration used in electroporation experiments with cells, i.e., 0.5–1.0 V transmembrane potential, and 10 μs–10 ms pulse duration [1,2]. Deviating from these conditions, several studies with skin have employed exponential-decay pulses of much longer duration (100 ms^{-1} s), which increases the amount of electrophoresis per pulse [4,15–18]. Compared to the short pulse protocols, these protocols also involved differences in pulse number and transdermal voltage: intermittent application of 'short' pulses lasted generally for an hour, in contrast, 'long' pulses were applied at lower voltages (>30 V) and only a few times. Although features of molecular transport due to these two protocols are similar, preliminary comparison in vitro suggested that greater transdermal transport could be achieved using long vs. short pulse protocols of similar transported charge [17,18].

Because the longer duration of the long pulses is expected to generate more heating (by the Joule effect) within SC aqueous pathways than the short pulses, safety issues become particularly relevant [19]. However, measurement of transepidermal water loss and erythema following the application of long pulses in vivo in hairless rats showed only small, transient increases that were similar in magnitude and duration to those caused by conventional iontophoresis, indicating that these protocols were well-tolerated [20].

Long, medium-voltage pulses might offer significant improvements over short, high-voltage pulses for transdermal drug delivery (e.g., fewer applications of pulses, increased transdermal transport), although they might involve greater technical requirement (e.g., larger capacitor needed, which could affect device size/energy) and increased potential for muscle stimulation [5,6]. In order to confirm the advantages of long pulses and improve our understanding of the effects of these two types of pulses on skin and transport, we have performed a systematic comparison, where the changes in the electrical properties of skin were assessed, transdermal transport was measured using the fluorescent molecule sulforhodamine, and the regions of transdermal molecular transport were observed [12,13,21].

2. Materials and methods

An experimental system was used that was based on a side-by-side permeation chamber with flow-through capability on the receptor side. It was designed for the simultaneous measurement of the transdermal transport of fluorescent molecules, in our case, sulforhodamine, and of the skin's passive electrical properties during automatically controlled high-voltage pulse application. The experimental approach has been reported previously [12,13,21], so

that only the main features of the methods will be presented here.

2.1. Skin preparation

Heat-separated human epidermis was used in all experiments. Tissue was obtained from human adult cadavers and frozen at −70°C until use. After heat-stripping, samples were stored at 4°C and 95% humidity, and were used within one week. To assure that initially there was intact skin barrier function, only skin samples that had at least 30 kΩ resistance (area≈0.7 cm^2) and exhibited a sulforhodamine (sr) flux below our detection limit (of the order of 10^{-2} $\mu g/cm^2$ h) [12] were used.

2.2. Permeation chamber

Human epidermis samples were clamped in a side-by-side flow-through permeation chamber (Crown Glass, Sommerville, NY, USA), with the SC facing the donor compartment. The compartments were filled with well-stirred 150 mM phosphate-buffered saline (NaCl, 138 mM; Na_2HPO_4, 8.1 mM; KH_2PO_4, 1.1 mM; KCl, 2.7 mM; Dulbecco's phosphate buffered saline, pH 7.4; Sigma, St Louis, MO, USA), the donor solution in addition containing sulforhodamine 101 (Sigma) at 1 mM. The chamber temperature was regulated to 37°C using a water-jacketed configuration [12].

2.3. Pulse application

In order to apply pulses, stainless steel electrodes protected by an agarose gel (2%; gel layer thickness≈0.5 cm; outer electrodes) were placed 3 cm from each side of the skin. The cathode and anode were in the donor and receptor compartments, respectively. A pulser (Electro Cell Manipulator 600, BTX, San Diego, CA, USA) that was modified to provide computer control, delivered exponential-decay pulse by discharging a capacitor.

A large number of experiments were carried out using exponential pulses with 'short' and 'long' pulse durations (Table 1). The long pulse time constant pulsing involved 20 pulses with a voltage applied across the electrodes ($U_{electrodes,0}$) of 100,

Table 1
Overview of the basic values measured for short time constant ($\tau_{pulse}=1$ ms) high-voltage ($U_{skin}\approx100$ V) and long time constant ($\tau_{pulse}=100$ ms) medium-voltage ($U_{skin}>30$ V) pulse protocols

Pulsing protocol[a]	$U^{b}_{skin,0}$ for first pulse (V)	R^{c}_{skin} during first pulse (Ω)	q^{d}_{tot} (C)	R^{e}_{skin} after 2 h (Ω)	Cumulative sulforhodamine transport ($\mu g/cm^2$[b])
240×(1000 V–1 ms)	99–127	40–86	0.54	3940	0.51–0.95
720×(1000 V–1 ms)	99–127	40–86	1.66	740–1650	6.28–9.20
240×(1500 V–1 ms)	76–156	24–78	0.81–0.87	130–450	3.75
720×(1500 V–1 ms)	76–156	24–78	2.24	Not measured	11.01–24.33
20×(100 V–100 ms)	41–45	415–490	0.11–0.25	14,400–34,500	0.54–0.57
20×(100 V–300 ms)	40–58	418	0.43–0.50	4090–4730	1.74–2.84
20×(200 V–100 ms)	68	224	0.54	1500	5.75
20×(200 V–300 ms)	48–62	166–208	1.40–1.67	1560	8.87–25.93
20×(300 V–100 ms)	63–68	114–124	0.85–0.92	1490–1510	7.20–7.98
20×(300 V–300 ms)	60–72	109–126	2.35–3.21	500–780	22.12–27.49
20×(400 V–100 ms)	69–85	84–113	1.32	1050	15.35
20×(400 V–300 ms)	68–96	85–136	2.52–4.46	180–1580	40.17–61.60

[a]Explanation of electrical protocol abbreviations is given in Section 2 of the text.
[b]$U_{skin,0}$ for first pulse, peak transdermal voltage for the first pulse of the protocol.
[c]R_{skin}, during first pulse, average skin resistance during the first pulse.
[d]q_{tot}, total charge transferred by the protocol.
[e]R_{skin}, after 2 h, skin dc-resistance 2 h after pulsing ceased. Prepulsed skin dc-resistance ranged between 30 and 100 kΩ. Results are presented as min–max. $n=1$ to 5.

200, 300 or 400 V, a pulse time constant (τ_{pulse}) of 100 or 300 ms and a pulse spacing of 6 min (2 h total). These protocols are typical of protocols previously reported [4,15–18]. In the case of the short pulse time constant protocols, the pulsing involved pulses with $U_{electrodes,0}$=1000 or 1500 V and τ_{pulse}=1 ms. To compensate for the much shorter individual pulse length, 20 'bursts' of 12 pulses were applied with 5 s pulse spacing, so that a pulse 'burst' had a duration of 1 min, which mimicked a single 'long pulse'. Each 'burst' was separated by 5 min, hence, the overall 'short pulse' pulsing protocol contained the main features of the 'long pulse' protocol (2 h total). Two more short pulse protocols, which were typical of protocols previously reported [3,22,23], were also used: pulses with either $U_{electrodes,0}$=1000 or 1500 V and τ_{pulse}=1 ms were spaced by 5 s for a total pulsing time of 1 h. Abbreviated descriptions of these electrical protocols are given in the tables [e.g., 20×(300 V–100 ms)] and provide, in order, the number of pulses applied (e.g., 20), $U_{electrodes,0}$ (e.g., 300 V) and τ_{pulse} (e.g., 100 ms).

2.4. Electrical measurements

The electrical behavior of the skin preparation was measured before, during and after each pulse by using a second pair of 'inner' electrodes [12,13]. These electrodes were constructed from Ag/AgCl (In-Vivo-Metric, Heraldsburg, CA, USA) and located 1 cm from the skin. Measurements allowed electrical behavior and skin resistance, R_{skin}, to be determined, with (1) measurements made before giving the prepulse value of R_{skin}, (2) measurements made during the pulse, reflecting the dramatic changes that are hypothesized to be due to electroporation and (3) measurements made after the pulse, partially indicating the degree of postpulse recovery.

During the application of the pulses, the outer electrodes were connected to the pulser, while the inner electrodes were connected to a high-voltage differential amplifier. The voltage across both of the inner electrodes for determination of the actual voltage across the skin, U_{skin}, and across a series resistance (5 Ω) for computation of the current [I(t)] was monitored by a digital oscilloscope (HP54601A, Hewlett Packard). In this way, U_{skin} and the apparent R_{skin} during the pulse were determined [13]. The total charge delivered through the skin by a pulsing protocol (q_{tot}) was calculated by time integrating I(t) for each pulse.

After a pulse, the high-voltage switch automatically disconnected the pulser and connected the inner electrodes to an impedance measurement system. The inner electrodes were placed in series with a measuring resistor (10^4 Ω) at the output of a generator (HP3112, Hewlett Packard), which delivered a small rectangular wave train with a 150-mV peak-to-peak amplitude. The resulting deformed wave train, which was measured across the electrodes with the oscilloscope, allowed computation of five elements of a skin equivalent electrical circuit, i.e., one resistance (R_{skin}) with two resistance–capacitance combinations in parallel. However, the most important changes were found for R_{skin}, the dc-part of the impedance and, thus, R_{skin} was used for further interpretation of the altered skin electrical properties due to the application of high-voltage [12,13].

2.5. Continuous transdermal flux measurements

Quantitative fluorescence measurements of sulforhodamine were carried out during the pulsing protocol, and for 2 h after pulsing. We used a continuous flow-through system: the contents of the receptor compartment were continuously flowed through a spectrofluorimeter (emission/excitation setting, 586/607 nm) allowing quasi-continuous determination of the receptor solution fluorescence (Fluorolog-2, model F112AI, SPEX Industries, Edison, NJ, USA). Deconvolution and calibration of the fluorescence measurements allowed calculation of the transdermal fluxes with a time resolution of about 1 min [12].

2.6. Transference number

The transference number, t_s, is the fraction of total current carried by the ionic species 's' [12,22]. The transference number of sulforhodamine (t_{sr}) during short and long pulse protocols was calculated using the equation:

$$t_{sr} = \frac{q_{sr}}{q_{tot}} \quad (1)$$

with $q_{sr}=M_{sr}z_{sr}F$, where M_{sr} is the moles of sulforhodamine transported during pulsing (median value from the data collected from the different skin samples), z_{sr} is the charge of sulforhodamine (-1) and F is Faraday's constant. The median value of q_{tot} was used.

The maximum value of t_{sr} occurs if sulforhodamine and small ion transports are all completely unhindered. In this case, their transport numbers scale with the product of electrophoretic mobility, concentration and charge. Because their mobilities are approximately equal, their relative concentrations were 1:300 (1 mM sulforhodamine and 300 mM small ions), and their relative charges were 1:1 ($z_{sr}=-1$ and generally $z_{ion}=-1$ or $+1$); the maximum value of t_{sr} would be approximately 3×10^{-3} [22].

2.7. Fractional aqueous area for transport

The combination of measuring the electrical properties of skin and sulforhodamine transport allows estimation of the fraction of skin that is available to small ions and to the transport of moderately sized molecules [12,22]. The fractional aqueous area for the transport of small ions was estimated using the equation [12]:

$$F_{w,ion}=\frac{\rho_{sal}h_{SC}}{A_{skin}R_{skin}} \quad (2)$$

where $\rho_{sal}=0.67\ \Omega\cdot m$, which is the specific resistance of saline, $h_{SC}=1.25\times10^{-5}$ m, which is the thickness of the stratum corneum [8], $A_{skin}=7\times10^{-5}$ m^2, which is the skin surface area and R_{skin} is the average apparent skin resistance during a pulsing protocol (median value).

By using $F_{w,ion}$ and t_{sr}, the fractional aqueous area available for the transport of sulforhodamine during pulsing ($F_{w,sr}$) was evaluated [12]:

$$F_{w,sr}=\frac{z_{ion}}{z_{sr}}\frac{[ion]}{[sr]}F_{w,ion}t_{sr} \quad (3)$$

where ([ion])/([sr]) is the relative concentration of the small ions and sulforhodamine.

2.8. Localized transport regions (LTRs)

After the acquisition of sulforhodamine flux data and the measurement of the electrical properties of skin following high-voltage pulse exposure, skin preparations were gently removed from the permeation chambers and rinsed with phosphate-buffered saline. They were then placed under a biocular fluorescence microscope (Olympus BH-2) and the transdermal transport regions for sulforhodamine were counted and characterized by size and shape [21].

2.9. Statistics

For each experimental condition, data from one to five skin preparations were collected. Representative individual skin sample data are presented (Figs. 1–4), or data were expressed as minimum–maximum values (Table 1) or were obtained from calculation (Figs. 5 and 6). Differences in median values between experimental conditions were assessed using the Mann-Whitney U-test ($p<0.05$).

3. Results

Experiments were carried out using short ($\tau_{pulse}=1$ ms), high-voltage ($U_{skin}\approx100$ V) pulses and long ($\tau_{pulse}\geq100$ ms), medium-voltage ($U_{skin}>30$ V) pulses (Table 1). A single typical experiment addressed the following quantities: the transdermal voltage, U_{skin}, the transdermal electrical resistance, R_{skin}, and the molecular flux. R_{skin} was measured before, during, between and after pulsing, which provided quantitative information about the transport of small ions, mainly Na^+ and Cl^- [12,13]. Simultaneous molecular flux measurements were carried out using sulforhodamine, a fluorescent molecule with a size of 607 g/mol and a charge of -1 [12]. Together, these experiments therefore show how transdermal transport depends on pulse magnitude, number and rate for small ions and a charged molecule of medium size.

3.1. Temporal behavior of U_{skin} and R_{skin} during a pulse

During a pulse, R_{skin} decreases by orders of magnitude while much smaller changes in resistance occur at the electrode/electrolyte interface, and still

smaller resistance changes occur within the bathing electrolyte. For this reason, U_{skin} was only a fraction of the voltage applied across the electrodes ($U_{electrodes}$), with this fraction depending on the value of R_{skin}. As higher voltages were applied, R_{skin} decreased further, making this fraction lower. In comparison with long time constant protocols, short time constant protocols involved larger $U_{electrodes}$, consequently, U_{skin} and R_{skin} were higher and lower, respectively (Table 1).

Fig. 1 shows a typical exponential decay of the voltage and the corresponding skin resistance time profile during a short and a long pulse. The short pulse with $U_{electrodes,0}=1500$ V and $\tau_{pulse}=1$ ms involved a maximum transdermal voltage of 127 V. Afterwards, the voltage decayed exponentially (Fig. 1a). Upon the pulse start, R_{skin} dropped by three orders of magnitude (from 50 kΩ to only 60 Ω) in less than a few microseconds, and then R_{skin} increased slightly for 4 ms. At time 4 ms, when U_{skin} reached approximately 8 V, R_{skin} strongly recovered to achieve its post-pulse value (Fig. 1a).

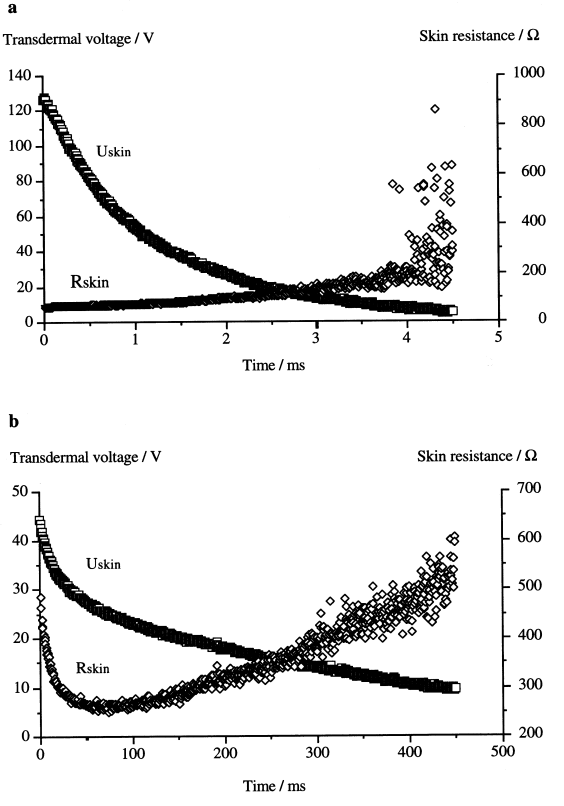

Fig. 1. Transdermal voltage ($U_{skin,0}$, □) and resistance (R_{skin}, ◇) (a) during a short pulse with $U_{electrodes,0}=1500$ V and $\tau_{pulse}=1$ ms, and (b) during a long pulse with $U_{electrodes,0}=100$ V and $\tau_{pulse}=300$ ms (data are from individual skin samples).

Transdermal voltage and resistance behavior during a longer lower voltage pulse is significantly different (Fig. 1b). Here, $U_{electrodes,0}$ was 100 V and τ_{pulse} 300 ms. U_{skin} showed two decay regions: U_{skin} started at 44 V and decreased to 25 V over approximately 75 ms; it then slowly decayed towards zero over the rest of the pulse (Fig. 1b). R_{skin} was consistent with U_{skin} behavior: two time regions could also be distinguished. R_{skin} initially dropped from 140 kΩ to about 485 Ω, but reached its minimal value of 250 Ω approximately 75 ms after the beginning of the pulse. From then until the end of the pulse, R_{skin} recovered towards its post-pulse value (Fig. 1b).

3.2. Transdermal electrical resistance

As illustrated in Fig. 1, the electrical behavior of the skin changed markedly during high-voltage pulsing. Fig. 2 describes the transdermal electrical resistance during, between and after a typical short and long time constant protocol. The short time constant protocol involved 20 bursts of 12 pulses with $U_{electrodes,0}=1000$ V and $\tau_{pulse}=1$ ms, applied at 6 min intervals (2 h total). $U_{skin,0}$ was 99 V for the first pulse. At the first pulse of the second burst, an important drop in $U_{skin,0}$ occurred. However, for all subsequent bursts, only a slight downward trend of $U_{skin,0}$ was evident (Fig. 2a). R_{skin} exhibited similar behavior (Fig. 2a). The resistance during the first pulse of the first burst was very low (45 Ω), and by the time of the second burst, the resistance was still much smaller. For the third through to the twentieth burst, a slight downward trend was also evident. The pre- and post-burst skin dc-resistances were also determined, with those 'immediately before' and 'immediately after' resistances providing an indication of the degree of recovery for each pulse (Fig. 2b). Compared to the pre-pulse value, the dc-resistance of skin was decreased by an order of magnitude after the first burst of 12 pulses, until the next group of pulses slight recovery took place. As pulsing progressed, the pre- and post-burst resistances de-

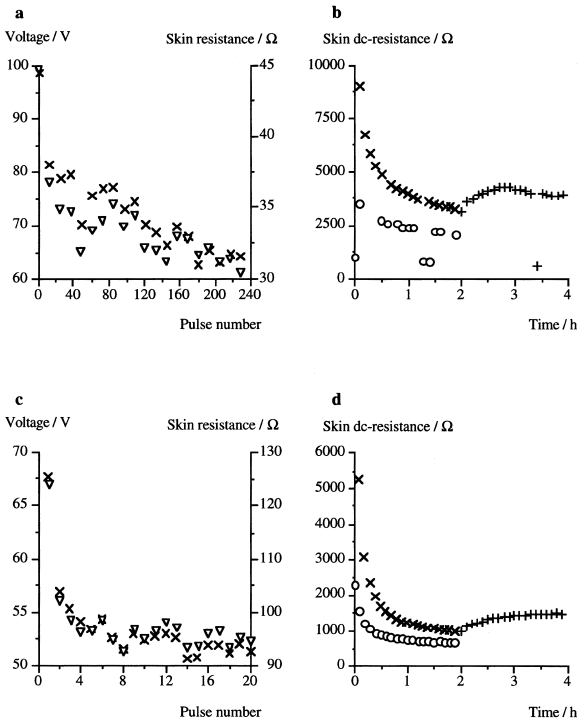

Fig. 2. (a) Peak transdermal voltage (X) and average resistance (▽) during the pulses of a representative short time constant pulse protocol: 240 pulses with $U_{electrodes}=1000$ V and $\tau_{pulse}=1$ ms were delivered; for the first minute, 12 pulses were separated by 5 s and then pulsing ceased for the next 5 min; this six minute pattern was repeated 20 times (2 h total). (b) Skin dc-resistance 6 ms after (○) and before each pulse (X) and for 2 h after (+) the same pulse series as in (a). Prepulse value of skin dc-resistance (>40 kΩ) is not shown for clarity. (c) and (d), as for (a) and (b), respectively, but for a typical long time constant pulse series i.e. $U_{electrodes}=300$ V, $\tau_{pulse}=100$ ms and a pulse spacing of 6 min. Data are from individual skin samples.

creased further, indicating that the skin became more permeable to ions. After the pulse series was terminated, the resistance rose slightly (Fig. 2b).

For comparison, a typical long pulse protocol is presented (Fig. 2c–d). In this case, the protocol involved the application of 20 pulses with $U_{electrode,0}=300$ V, $\tau_{pulse}=100$ ms and a 6-min pulse spacing (2 h total). The electric behavior during and between/after pulsing was qualitatively similar to the case of the short time constant pulsing protocol (Fig. 2). The peak transdermal voltage fell strongly from the first to the second pulse, but only slightly for subsequent pulses. R_{skin} behavior during the pulse series followed a similar profile (Fig. 2c). A few hours following long pulses as well as following short pulses, R_{skin} recovered by at least one order of magnitude (Fig. 2, Table 1; short vs. long pulses, $p>0.05$).

3.3. Transdermal transport

For the same total charge transferred, the long pulses provided higher transport of sulforhodamine than the short pulses. For both protocols, however, the amounts of molecule transported generally increased with the voltage, duration and/or number of pulses (Table 1).

Transdermal molecular fluxes vs. time are shown in Figs. 3 and 4 for typical short and long time constant protocols. The short pulse burst protocols can be directly compared to the long pulse protocols. To mimic the long pulse protocol and in order to provide comparable electrical charge transferred, groups of twelve short pulses were applied at 6 min intervals. Before pulsing, passive transdermal transport of sulforhodamine was lower than our detection

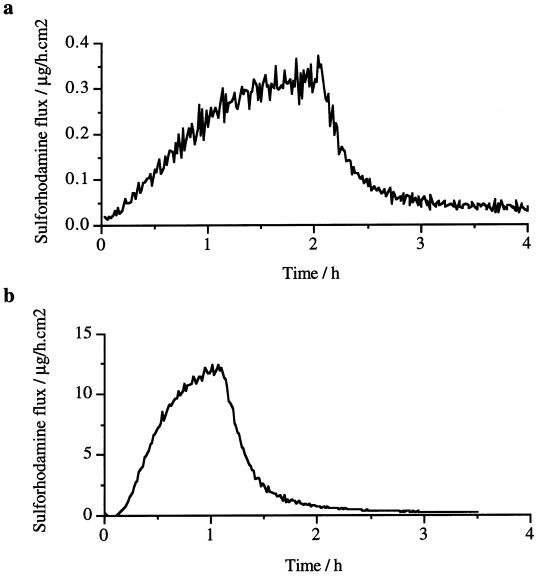

Fig. 3. Sulforhodamine flux vs. time due to typical short time constant pulse protocols (data are from individual skin samples). (a) 20 bursts of 12 pulses with $U_{electrodes}=1000$ V, $\tau_{pulse}=1$ ms, a pulse spacing of 5 s and burst spacing of 6 min (2 h total). (b) 720 pulses with $U_{electrodes}=1500$ V, $\tau_{pulse}=1$ ms and a pulse spacing of 5 s (1 h total).

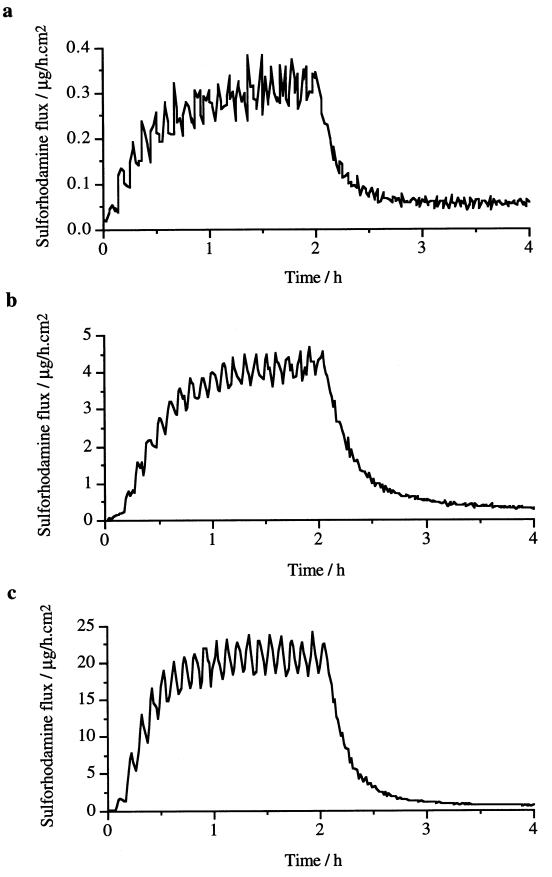

Fig. 4. Sulforhodamine flux vs. time due to typical long time constant pulse protocols (data are from individual skin samples). (a) 20 pulses with $U_{electrodes}=100$ V, $\tau_{pulse}=100$ ms and a pulse spacing of 6 min (2 h total). (b) 20 pulses with $U_{electrodes}=300$ V, $\tau_{pulse}=100$ ms and a pulse spacing of 6 min (2 h total). (c) 20 pulses with $U_{electrodes}=400$ V, $\tau_{pulse}=300$ ms and a pulse spacing of 6 min (2 h total).

limit. Initially, due to the first burst of short pulses, negligible sulforhodamine transport occurred. As the short pulse series progressed, sulforhodamine flux increased further. Increases of up to two orders of magnitude were achieved in sulforhodamine fluxes using bursts of short pulses protocols (Fig. 3a). However, on increasing the pulse rate, i.e., when pulsing at one pulse per 5 s for 1 h, increases of up to three orders of magnitude in molecular fluxes could be achieved (Fig. 3b). After the pulses, sulforhodamine flux decreased. However, 2 h after pulsing, sulforhodamine efflux was still significant (Fig. 3).

Qualitative and quantitative differences in molecular transport due to long vs. short pulses were apparent (Figs. 3 and 4). Onset fluxes as well as maximum fluxes of sulforhodamine were higher following long medium-voltage pulses than following bursts of short high-voltage pulses ($p<0.05$). In contrast with short time constant protocols, molecular fluxes due to long pulses increased up to a maximum and then plateaued. Also, flux decreases between pulses appeared. Increases in sulforhodamine fluxes of up to three–four orders of magnitude could be achieved. Passive fluxes after pulsing were the same as those following short pulses ($p>0.05$). Similar to short pulses, increasing pulse voltage, rate and/or number increased transdermal transport (Fig. 4, Table 1).

3.4. Transference numbers

Transference numbers of sulforhodamine (t_{sr}) during long pulse protocols were generally three times greater than during short pulse protocols (Fig. 5a; short vs. long pulses, $p<0.05$). As reported previously, t_{sr} tended to increase with the voltage and the number of short pulses (Fig. 5b) [12,22]. t_{sr} did not increase significantly with the length of long pulses ($p>0.05$), however, it did increase on increasing the voltage from 100 to 200 V and afterwards plateaued (Fig. 5c). The highest values reached by t_{sr} were only a third of the maximum values possible (see Section 2; [22]).

3.5. Fractional aqueous area for transport

The fractional aqueous area available for small ion transport, mainly Na^+ and Cl^- ($F_{w,ion}$), of unpulsed skin preparation has been estimated to be 10^{-6} [13]. When pulsing, $F_{w,ion}$ increased by up to three orders of magnitude (Fig. 6a). Consistent with the larger drop in R_{skin} during short vs. long pulses (Table 1 and Fig. 1), $F_{w,ion}$ was higher during short pulses of high voltage ($p<0.05$; Fig. 6a).

The fractional aqueous areas for sulforhodamine ($F_{w,sr}$) transport were smaller than $F_{w,ion}$ (Fig. 6b; $p<0.05$). Because sulforhodamine is larger than Na^+ and Cl^-, its transport in the aqueous pathways is probably more hindered, making the effective area for transport smaller [13]. $F_{w,sr}$ was similar regard-

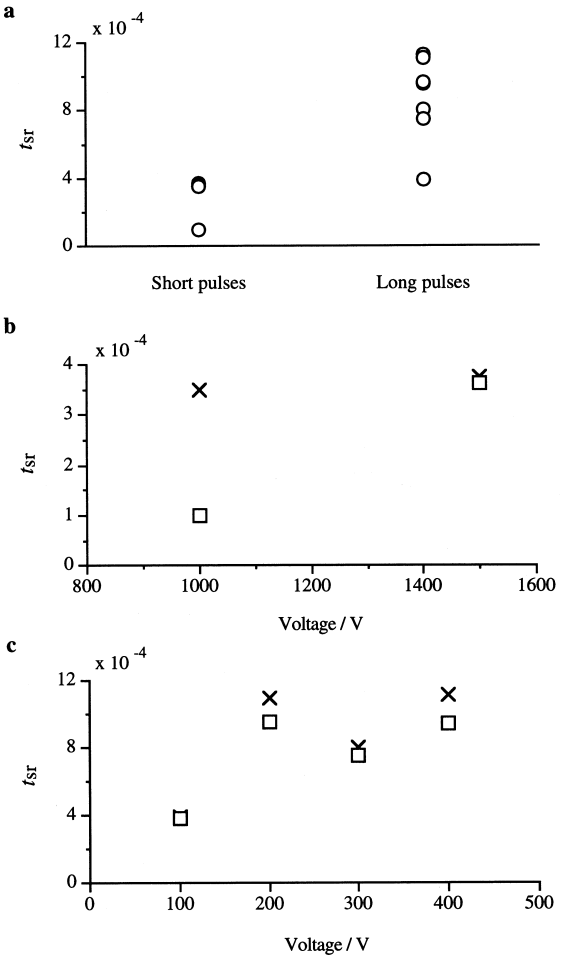

Fig. 5. (a) Sulforhodamine transference numbers, t_{sr}, during short and long pulse protocols. (b) t_{sr} vs. applied voltage of short pulse protocols; 240 (□) or 720 (X) pulses were applied. (**c**) t_{sr} vs. applied voltage of long pulse protocols, pulses of 100 (□) or 300 ms (X) were applied.

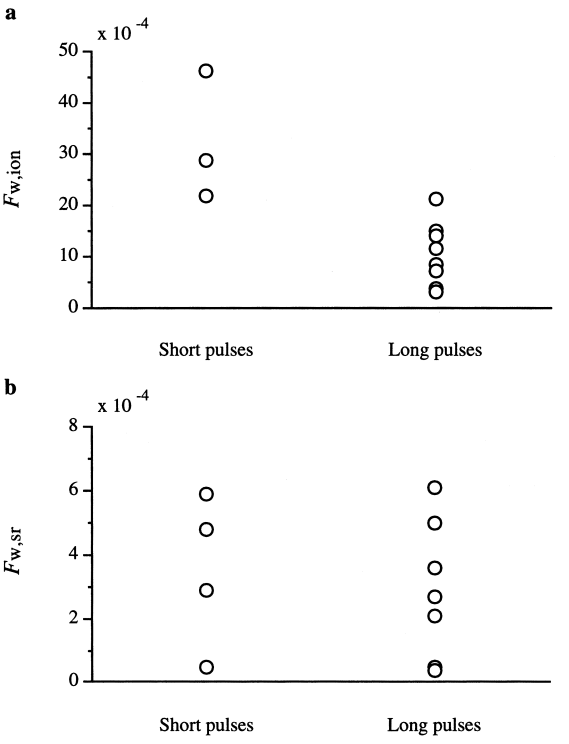

Fig. 6. Fractional aqueous areas for small ions ($F_{w,ion}$, a) and for sulforhodamine ($F_{w,sr}$, b) transport during short and long pulse protocols.

less of whether short or long pulse protocols were applied (Fig. 6b; $p>0.05$).

3.6. Localized transport regions

Previous imaging studies reported that transdermal transport due to high-voltage pulses is highly concentrated into localized transport regions (LTRs) of the SC. These LTRs were not located at the appendages or the rete pegs of the skin and molecular transport within an LTR occurred mainly through transcellular pathways [21,23].

In this study, we counted and characterized by size and shape the LTRs of sulforhodamine due to short and long high-voltage pulses. The LTRs due to the 1 ms pulses had a diameter of approximately 100–300 μm and were, as reported previously, randomly distributed over the stratum corneum (Table 2) [21]. They were of similar size regardless of the pulse voltage or number, however, their number seemed to increase with both pulse voltage and number. As found for the short pulses, sulforhodamine transport due to long pulses was concentrated within LTRs, but here, strikingly, the size of the LTRs was an order of magnitude larger and their number an order of magnitude smaller ($p<0.05$, short vs. long pulses; Table 2). Moreover, in contrast with the short pulses case, the LTRs often included an appendage, apparently randomly localized inside the LTR. A slight trend towards greater LTRs with higher voltage and with 300 vs. 100 ms ($p>0.05$) pulses was apparent (Table 2). As in the short pulse case, the number of

Table 2
Size and number of localized transport regions (LTRs) of sulforhodamine following short time constant ($\tau_{pulse}=1$ ms) high-voltage ($U_{skin}\sim100$ V) and long time constant ($\tau_{pulse}=100$ms) medium-voltage ($U_{skin}>30$ V) pulse protocols

Pulsing protocol[1]	Size (diameter in mm)	Number (per 0.1 cm^2)
240×(1000 V–1 ms)	0.1–0.3	26
720×(1000 V–1 ms)	0.1–0.3	40–80
240×(1500 V–1 ms)	0.1–0.2	60
720×(1500 V–1 ms)	0.1–0.3	70–90
20×(100 V–100 ms)	No LTRs	
20×(100 V–300 ms)	0.8	Rare
20×(200 V–100 ms)	0.4–0.8	Not measured
20×(200 V–300 ms)	0.5–1.0	2
20×(300 V–100 ms)	0.2–0.6	6
20×(300 V–300 ms)	0.5–0.8	6
20×(400 V–100 ms)	0.6–1.5	10
20×(400 V–300 ms)	1.0–2.5	8

[a]See Section 2 for explanation of the electrical protocol abbreviations.

LTRs increased with the pulse voltage, and no effect of the pulse length was evident. A more complete description of LTRs associated with short and long pulses is presented elsewhere [24].

4. Discussion

This study demonstrates that short high-voltage and long medium-voltage pulses induce the same types of important events within the multilamellar stratum corneum (SC): dramatic changes in the electrical properties of skin and significant increases in transdermal transport occur through localized regions of the SC (Figs. 1–6, Tables 1 and 2). However, it also indicates that short and long pulses alter skin properties in ways that are qualitatively and quantitatively different. Moreover, the results provide insight into the influence of the nature of the pulses on the relative number, size and evolution of the aqueous pathways created by the electric field.

Most importantly, long medium-voltage pulses appeared to be more efficient in promoting transport across skin than short high-voltage pulses, and this might be especially true for large compounds (e.g., heparin, therapeutic proteins). The efficiency with which an electric current transports a compound across skin can be evaluated using transport variables combined with electrical measurements, e.g., onset time for significant transport, transference number and fractional aqueous area available for transport [12,22]. At the time of the first long pulse, significant sulforhodamine transport appeared, whereas negligible transport occurred due to the first burst of short pulses transporting the same amount of charges. It is only at the time of the second burst of short pulses that significant transport was apparent (Figs. 3 and 4). Long pulses yielded transference numbers of sulforhodamine that were three-fold higher than those obtained using short pulses (Fig. 5). When considering the fractional aqueous area available for ionic transport, $F_{w,ion}$ involved 0.2 to 0.5% of the skin surface area during short pulse protocols, whereas during long pulse protocols, it involved 0.03 to 0.2%. However, the fractional aqueous area available for molecular transport, $F_{w,sr}$, was similar when either short or long pulses were applied (Fig. 6).

Together, these data suggest that long pulses may involve the creation of fewer but larger aqueous pathways and/or aqueous pathways with less steric hindrance, such that more of the aqueous pathways were involved in the transport of the charged moderately sized fluorescent molecule. By comparing $F_{w,ion}$ to $F_{w,sr}$, it can be estimated that 2 to 13% of the aqueous pathways created by short high-voltage pulses were involved in sulforhodamine transport, while during long medium-voltage pulses, this fraction ranged from 13 to 33% (Fig. 6). This was similarly observed with cells and artificial planar bilayer membranes, where longer pulses were associated with larger pores [1,2,25]. The history of the voltage across the lipid-based barrier of the skin, i.e., the SC, determines, according to our hypothesis, the creation and evolution of aqueous pathways and, therefore, the fractional aqueous area available to a particular ionic or molecular species.

The current flow through the skin associated with electroporation was theoretically predicted to raise the skin temperature at localized sites of transport, especially in the case of long pulses [19]. Localized ohmic heating was confirmed by experiments where the peak temperature rise reached approximately 20°C when pulses of 1 ms and 100 V were applied across the skin and up to 50°C for 300 ms, 60 V pulses [26]. It might be suggested that the associated

increase in permeability due to long pulses could be the result of a further, secondary, morphological transformation of the SC caused by the rise in temperature. A high enough temperature rise could disrupt the structure of the SC and hence its normal barrier function by endothermic transformation of the lipids.

Sulforhodamine flux increased progressively with each additional pulse of the short pulse series. In contrast, during long time constant pulsing, after reaching a maximum, the sulforhodamine flux plateaued (Figs. 3 and 4). However, as both short and long pulsing progressed, R_{skin} decreased slightly, indicating further creation and/or expansion of aqueous pathways (Fig. 2). Hence, this suggests that new pathways created by later short pulses would be larger than those created by the first pulses and/or that pathways created by the first short pulses would be enlarged by later ones [22]. In contrast, the size of the pathways created by the long pulses seemed to plateau quickly. Within each pulsing category, increasing the pulse voltage, duration and/or number generally increased the sulforhodamine transference number, showing that an increase in any of the pulse parameters might be a way to achieve larger aqueous pathways (Fig. 5).

The charged water-soluble molecule, sulforhodamine, experiences negligible transport in the absence of aqueous pathways (Figs. 3 and 4) [12]. At high-voltage, we expect the pulses not only to create aqueous pathways, but also to provide a local driving force for the transport of charged molecules by electrophoresis [1–4]. In addition to electrophoresis during a pulse, passive transport between pulses through long-lasting pathways and release from a reservoir created within the skin should, however, also be considered [4,27]. Because decreases in sulforhodamine fluxes between short vs. long pulses were weaker, the contribution of transdermal transport by diffusion between pulses and/or the skin storage/release of sulforhodamine during short time constant pulsing might be more important (Figs. 3 and 4).

The LTRs of sulforhodamine due to short and long pulses were strikingly different. The size of the LTRs was an order of magnitude greater and their number an order of magnitude smaller for long than for short pulses (Table 2). Basically, the size depended on pulse length while the number depended on pulse voltage. This suggests that LTRs might expand during the pulse while the magnitude of the voltage determines which regions of the SC are susceptible to electroporation i.e., the higher the voltage, the greater the number of regions reaching the threshold voltage [21–23]. LTRs associated with short and long pulses are further discussed in a companion paper [24].

The behavior of R_{skin} followed a similar profile during and for 2 h after pulsing for the short and long pulses, indicating similar alteration and recovery processes of the skin (Fig. 2). Three recovery phases could be distinguished [13]. Upon the start of a short or long pulse, R_{skin} dropped by three and two orders of magnitude, respectively (Table 1, Figs. 1 and 2). A first phase of recovery occurred at the end of the pulse: R_{skin} was increased by one–two orders of magnitude after the pulse (Fig. 2). Until the application of the next pulse, R_{skin} exhibited a second recovery process: resistance generally increased by a factor one–two (Fig. 2). Finally, a third and still weaker and slower recovery phase took place after pulsing ceased (Fig. 2). While a dramatic and rapid drop in resistance during pulsing is a hallmark of pathway creation [1,2], post-pulse resistance might reflect pathway resealing with water/ion entrapment [28].

5. Conclusion

Understanding and optimization of molecular transport due to high-voltage pulses have to be addressed before transdermal drug delivery using electroporation may find clinical application. Two main pulse protocols have been employed to promote transport across skin: i.e., the intermittent application of short high-voltage pulses and a few applications of long medium-voltage pulses. Here, we compared these two protocols in terms of changes in the electrical properties of skin and transdermal transport. Whereas both protocols induced similar alteration and recovery processes of skin electrical resistance, long pulses of medium-voltage appeared to be more efficient in transporting molecules across skin. This was demonstrated by the shorter onset time for molecular transport, the higher transference number

and the increased fraction of aqueous pathways created/involved in molecular transport due to long pulse protocols.

Acknowledgements

We thank T.E. Vaughan and M.R. Prausnitz for helpful discussions. This work was supported by NIH grant ARH4921 and Whitaker Foundation grant RR10963. R. Vanbever was supported by a travel grant from the Fonds National de la Recherche Scientifique (FNRS, Belgium). Prof. V. Préat is Senior Research Associate, FNRS (Belgium).

References

[1] D.C. Chang, B.M. Chassy, J. Saunders, A. Sowers (Eds.), Guide to Electroporation and Electrofusion, Academic Press, New York, 1992.
[2] J.C. Weaver, Y.A. Chizmadzhev, Theory of electroporation: a review, Bioelectrochem. Bioenerget. 41 (1996) 135–160.
[3] M.R. Prausnitz, V.G. Bose, R. Langer, J.C. Weaver, Electroporation of mammalian skin: a mechanism to enhance transdermal drug delivery, Proc. Natl. Acad. Sci. USA 90 (1993) 10504–10508.
[4] R. Vanbever, N. Lecouturier, V. Préat, Transdermal delivery of metoprolol by electroporation, Pharm. Res. 11 (1994) 1657–1662.
[5] M.R. Prausnitz, A practical assessment of transdermal drug delivery by skin electroporation. Adv. Drug Deliv. Rev. (in press).
[6] R. Vanbever, V. Préat, In vivo efficacy and safety of skin electroporation. Adv. Drug Deliv. Rev. (in press).
[7] J.C. Weaver, T.E. Vaughan, Y. Chizmadzhev, Theory of electrical creation of aqueous pathways across skin transport barriers. Adv. Drug Deliv. Rev. (in press).
[8] J. Hadgraft, R.H. Guy (Eds.), Transdermal Drug Delivery — Development Issues and Research Initiatives, Marcel Dekker, New York, 1989.
[9] E.W. Smith, H.I. Maibach (Eds.), Percutaneous Penetration Enhancers, CRC Press, Boca Raton, FL, 1995.
[10] R. Langer, Drug delivery and targeting, Nature 392 (1998) 5–10.
[11] T. Chen, E.M. Segall, R. Langer, J.C. Weaver, Skin electroporation: rapid masurements of the transdermal voltage and flux of four fluorescent molecules show a transition to large fluxes near 50 V, J. Pharm. Sci. 37 (1998) 1368–1374.
[12] U.F. Pliquett, J.C. Weaver, Electroporation of human skin: Simultaneous measurement of changes in the transport of two fluorescent molecules and in the passive electrical properties, Bioelectrochem. Bioenerget. 39 (1996) 1–12.
[13] U.F. Pliquett, R. Langer, J.C. Weaver, Changes in the passive electrical properties of human stratum corneum due to electroporation, Biochim. Biophys. Acta 1239 (1995) 111–121.
[14] D. Bommannan, J. Tamada, L. Leung, R.O. Potts, Effect of electroporation on transdermal iontophoretic delivery of luteinizing hormone releasing hormone (LHRH) in vitro, Pharm. Res. 11 (1994) 1809–1814.
[15] A. Jadoul, H. Tanajo, V. Préat, F. Spies, H. Boddé, Electroperturbation of human stratum corneum fine structure by high voltage pulses: A freeze fracture electron microscopy and differential thermal analysis study. J. Invest. Derm. (in press).
[16] V. Regnier, T. Le Doan, V. Préat, Parameters controlling topical delivery of oligonucleotides by electroporation, J. Drug Target. 5 (1998) 275–289.
[17] R. Vanbever, V. Préat, Factors affecting transdermal delivery of metoprolol by electroporation, Bioelectrochem. Bioenerg. 38 (1995) 223–228.
[18] R. Vanbever, E. Le Boulengé, V. Préat, Transdermal delivery of fentanyl by electroporation I. Influence of electrical factors, Pharm. Res. 13 (1996) 559–565.
[19] G. Martin, U.F. Pliquett, J.C. Weaver, Theoretical analysis of localized heating in human skin subjected to 'high-voltage' pulses (submitted).
[20] R. Vanbever, D. Fouchard, A. Jadoul, N. De Morre, V. Préat, J.-P. Marty, In vivo non-invasive evaluation of hairless rat skin after high-voltage pulse exposure, Skin Pharmacol. Appl. Skin Physiol. 11 (1998) 23–24.
[21] U.F. Pliquett, T.E. Zewert, T. Chen, R. Langer, J.C. Weaver, Imaging of fluorescent molecule and small ion transport through human stratum corneum during high-voltage pulsing: localized transport regions are involved, Biophys. Chem. 58 (1996) 185–204.
[22] M.R. Prausnitz, C.S. Lee, C.H. Liu, J.C. Pang, T.P. Singh, R. Langer, J.C. Weaver, Transdermal transport efficiency during skin electroporation and iontophoresis, J. Control. Release 38 (1996) 205–217.
[23] M.R. Prausnitz, J.A. Gimm, R.H. Guy, R. Langer, J.C. Weaver, C. Cullander, Imaging of transport pathways across human stratum corneum during high-voltage and low-voltage exposures, J. Pharm. Sci. 85 (1996) 1363–1370.
[24] U.F. Pliquett, R. Vanbever, V. Préat, J.C. Weaver, Local transport regions (LTRs) in human stratum corneum due to long and short 'high-voltage' pulses. Bioelectrochem. Bioenerg. (in press).
[25] S.A. Freeman, M.A. Wang, J.C. Weaver, Theory of electroporation of planar bilayer membranes: predictions of the aqueous area, change in capacitance, and pore–pore separation, Biophys. J. 67 (1994) 42–56.
[26] U.F. Pliquett, G.T. Martin, J.C. Weaver, Kinetics of the temperature rise within human stratum corneum during electroporation and pulsed high-voltage iontophoresis (submitted).

[27] R. Vanbever, N. De Morre, V. Préat, Transdermal delivery of fentanyl by electroporation. II. Mechanisms involved in drug transport, Pharm. Res. 13 (1996) 1360–1366.
[28] R. Vanbever, D. Skrypczak, A. Jadoul, V. Préat, Comparison of skin electroperturbations induced by iontophoresis and electroporation, in: K.R. Brain, V.J. James, K.A. Walters (Eds.), Prediction of Percutaneous Penetration, vol. 4b, Cardiff, 1995, pp. 243–246.